Broadband Spectrum Sensing of Distributed Modulated Wideband Converter Based on Markov Random Field

Zhi Li, Jiawei Zhu, Ziyong Xu and Wei Hua

The Distributed Modulated Wideband Converter (DMWC) is a networking system developed from the Modulated Wideband Converter, which converts all sampling channels into sensing nodes with number variables to implement signal undersampling. When the number of sparse subbands changes, the number of nodes can be adjusted flexibly to improve the reconstruction rate. Owing to the different attenuations of distributed nodes in different locations, it is worthwhile to find out how to select the optimal sensing node as the sampling channel. This paper proposes the spectrum sensing of DMWC based on a Markov random field (MRF) to select the ideal node, which is compared to the image edge segmentation. The attenuation of the candidate nodes is estimated based on the attenuation of the neighboring nodes that have participated in the DMWC system. Theoretical analysis and numerical simulations show that neighboring attenuation plays an important role in determining the node selection, and selecting the node using MRF can avoid serious transmission attenuation. Furthermore, DMWC can greatly improve recovery performance by using a Markov random field compared with random selection.

Keywords: Cooperative spectrum sensing, Distributed modulated wideband converter, Markov random field, Node selection, Recovery performance, Transmission attenuation.

Manuscript received June 28, 2017; revised Dec. 6, 2017; accepted Feb. 24, 2018.

Zhi Li (corresponding author, lizhi@scu.edu.cn), Jiawei Zhu (scuzhujiawei@163.com), Ziyong Xu (scuxuzhiyong@163.com), and Wei Hua (huaw@scu.edu.cn) are with the College of Electronics and Information Engineering, Sichuan University, Chengdu, China.

I. Introduction

Cognitive radio is considered a potential technology that can drastically enhance the real-time utilization of the target frequency range [1], [2]. It allows second users (SUs) to monitor the frequency range that has been assigned to the primary users (PUs) and to search the spectrum hole to access. However, as the target frequency range increases, the traditional methods that are applied to low frequencies become impractical. Owing to the wide spectral range, the first problem to be solved is the limitation of the Nyquist sampling rate.

Fortunately, several sub-Nyquist sampling methods have recently been proposed to overcome this difficulty. The modulated wideband converter (MWC) is the most typical method. It was first proposed by Eldar [3]–[5]. It is a kind of analog sub-Nyquist sampling system with several sampling channels, and it reconstructs the broadband signal using compressed sensing (CS), which was proposed in [6]. However, MWC has no adaptive mechanism for a signal time-varying support set. It is difficult for the hardware circuit design to adjust the number of sampling channels under the given sparsity. The recovery performance will be reduced when the number of sparse bands increases.

A distributed modulated wideband converter (DMWC) can handle these difficulties dynamically. By combining the characteristics of a broadband cooperative spectrum sensing network [7], [8], the DMWC changes the channels into some distributed sensing nodes as virtual undersampling channels [9]. The number of nodes can be adjusted according to the time-varying support set. Considering the unavoidable factors in practical application, the DMWC takes the transmission attenuation and phase shift into account in every input node. The transmission attenuation can prevent recovery performance, so selecting the optimal sensing node as the sampling channel is an essential issue.

In this paper, we propose the spectrum sensing of a DMWC based on a Markov random field (MRF) to select the optimal node. Facing the time-dependent support set problem, the DMWC needs to adjust the number of virtual sampling channels by adding the sensing nodes. In the time domain, the transmission attenuation at the next time is closely related to the current time, and the relationship with the past moment weakens gradually. In the spatial domain, there is a correlation between the attenuation of successive adjacent nodes, which is satisfied with local statistical characteristics.

It can be seen that the transmission attenuation of adjacent distributed nodes satisfies the characteristics of the Markov random field [10], [11]. Therefore, we introduce the MRF as the selection method. A first-order neighborhood system is modeled by all nodes in the sensing region. Then, we introduce a self-weight coefficient and a cross-weight coefficient to the energy function according to prior knowledge. Conditional probability is constructed proportionally to measure the possibility of node selection. The selected probability of the candidate nodes is estimated based on the attenuation and distance of the neighboring nodes that have participated in the DMWC system. Theoretical analysis and numerical simulations show that neighboring attenuation plays an important role in determining the node selection. Furthermore, the DMWC can greatly improve the quality of node selection by using a Markov random field compared with random selection.

This paper is organized as follows. In Section II, we present the theoretical background of the DMWC and discuss the motivation behind the node selection. In Section III, we describe the node selection based on a Markov random field. Section IV shows the numerical simulations and results.

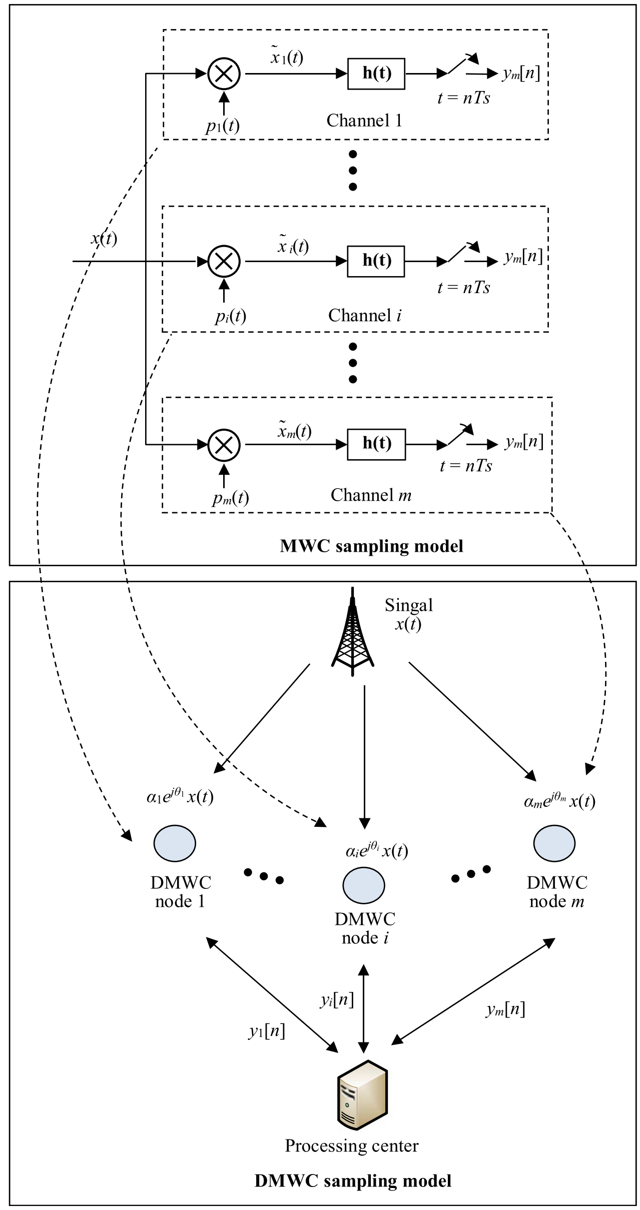

Fig. 1. Comparative map of MWC and DMWC.

II. Background and Motivation

The DMWC framework is similar to that of the MWC, but it takes phase shift and transmission attenuation into account in each channel, as depicted in Fig. 1 [12]. Each node conducts one-channel sampling with a mixer, a low-pass filter, and a low-speed analog-to-digital conversion independently. Then, all of the sampling data are transmitted to the processing center to complete the recovery uniformly.

Assuming that the transmission signal of the base station is $x(t)$, the received signal $x_i(t)$ of the i-th node must be different with regard to the phase shift and transmission attenuation owing to the different geographical locations. For the processing center, the geographical location of each node is known, that is, d_i is prior knowledge. According to prior knowledge, let θ_i be the phase shift of $x_i(t)$ relative to $x(t)$. The phase shift θ_i is calculated by

$$\theta_i = \frac{2\pi d_i}{CT}, \tag{1}$$

where C represents the transmission speed of the signal, and $1/T$ represents the bandwidth of $x(t)$. Further, let α_i denote the attenuation coefficient of $x_i(t)$ relative to $x(t)$. The greater the attenuation coefficient α_i, the smaller the

https://doi.org/10.4218/etrij.2017-0028

degree of transmission attenuation. The attenuation coefficient α_i is calculated by

$$\alpha_i = \frac{P_a}{P_t} = \frac{G\lambda^2}{(4\pi)^2 d_i^2 F}, \quad (2)$$

where P_a is the received power, P_t is the transmission power, G is the system gain, and F denotes the system loss factor. When considering the phase shift and the transmission attenuation, the input signal of the i-th virtual sampling channel in the DMWC can be expressed as

$$x_i(t) = \alpha_i e^{j\theta_i} x(t), \quad (3)$$

where $\theta_i \in [0, \pi/2]$ and $\alpha_i \in [0, 1]$.

After the signal $x_i(t)$ passes through the mixer and low-pass filter, the signal spectrum is moved to the baseband. The final output sequence $y_i[n]$ of the i-th channel has a discrete-time Fourier transform [9]:

$$\begin{aligned} Y_i(e^{j2\pi f T_s}) &= \sum_{n=-\infty}^{+\infty} y_i[n] e^{-j2\pi f n T_s} \\ &= \sum_{l=-L_0}^{+L_0} \alpha_i e^{j\theta_i} c_{il} X(f - l f_p), f \in \left[\frac{-f_s}{2}, \frac{f_s}{2}\right]. \end{aligned} \quad (4)$$

We can recover the signal $X(f)$ from $y_i[n]$ according to (4). Changing (4) into its matrix form occurs as

$$y(f) = \mathbf{A} z(f), f \in \left[\frac{-f_s}{2}, \frac{f_s}{2}\right], \quad (5)$$

where matrix $\mathbf{A}$ contains the element a_{il}:

$$a_{il} = \alpha_i e^{j\theta_i} c_{il}^*. \quad (6)$$

Equation (5) is a link between the DMWC and CS. Reference [3] uses a continuous-to-finite (CTF) block to recover the support set, which is combined with the recovery algorithm orthogonal matching pursuit (OMP). The recovery process is transformed into the following optimization problem:

$$\hat{z}(f) = \min ||z(f)||_0 \text{ s.t.} ||\mathbf{A} z(f) - y(f)||_2^2 < \eta, \quad (7)$$

where η is the maximal acceptable error rate.

In order to obtain a reliable signal recovery support set, the DMWC and MWC need a restriction mechanism for the number of undersampled channels. Reference [3] pointed out the necessary conditions for obtaining a reliable support set as follows:

$$m \geq 2N, \quad (8)$$

where m is the number of channels, and N is the number of subbands. If (8) cannot be satisfied, this will result in measurement matrix rank($\mathbf{A}$) $\leq m$. This means that there exist two different N-sparse vectors satisfying the constraint condition. This is clearly unreliable.

As shown in [9], the random phase shift between the virtual channels has a weak effect on the recovery of the support set. However, the transmission attenuation factor is opposite to the random phase shift. When the transmission attenuation becomes more serious, it will greatly damage the joint sparse characteristics between the channels and weaken the noncorrelation between the columns of the measurement matrix. This results in the degradation of the support set and a reduction in the recovery probability of spectrum sensing.

In addition, when facing time-varying support set problems, the recovery performance can be improved by increasing the number of cooperative nodes. Equation (8) measures the number of channels that ensures reliable support, which is also the basis for determining the number of distributed nodes participating in the DMWC. In addition, when the input SNR is too low, the processing center can appropriately increase the number of sensing nodes to improve the recovery performance. However, the method for selecting an optimal sensing node as the sampling channel for the DMWC is worthy of consideration [13], [14].

III. Node Selection Based on MRF

For a time-varying support set, the DMWC must dynamically increase the number of sensing nodes to ensure a sufficient undersampling channel. In order to obtain a higher reconstruction rate of the support set, transmission attenuation coefficient α_i must be as large as possible. Thus, we introduce the Markov random field as an optimization scheme of the DMWC sensing node selection for the following reasons: In the time domain, the transmission attenuation at the next time is closely related to the current time, and the relationship with the past moment weakens gradually. In the spatial domain, there is a correlation between the attenuation of successive adjacent nodes, which is satisfied with local statistical characteristics.

It can be seen that the transmission attenuation of adjacent distributed nodes satisfies the characteristics of the Markov random field. In addition, the pixel values of the adjacent pixel groups of the image satisfy the Markov random field. As an analogy to image edge segmentation [11], the distributed sensing nodes are like the pixels of an image, and the attenuation coefficient is the pixel value. These lay the model foundation for the introduction of the MRF.

1. Related Theory of MRF

The neighborhood is an important concept in a Markov random field. A set of nodes $\{\delta(r), r \in R\}$ in a two-dimensional space $\boldsymbol{R}$ satisfies

$$\begin{cases} \delta(r) \subset \boldsymbol{R} \\ r \notin \delta(r) \\ s \in \delta(r) \end{cases}, \tag{9}$$

where $s \in \delta(r)$ are the neighboring nodes of the center node r. $\delta(r)$ is the neighboring set of the center point r. The neighborhood system can be defined as [10]

$$\delta^{(k)}(r) = \{s|d(r,s) \leq k, s \neq r\}. \tag{10}$$

Here, k is the order of the neighborhood system, s is the neighboring points, and $\delta(r)$ is the neighboring set of the center point r. d (r, s) represents the Euclidean distance from the center point r to the neighboring point s. The positional relationship between the points in the hierarchical neighborhood system is shown in Fig. 2.

The distribution probability of the Markov random field can be described by the Gibbs distribution [15], and its probability function is

$$P(X = x) = \frac{1}{Z} e^{-U(x)}, \tag{11}$$

where $U(x) = -\sum V_c(x)$ represents the energy function, $V_c(x)$ is the potential function of the subgroup c in the neighborhood system, and $Z = \sum e^{-U(x)}$ is a normalized constant. Solving practical problems using a Markov random field can be attributed to the study of the energy function. Therefore, designing an energy function that meets the requirements is the most critical task in introducing the MRF to a practical application scenario.

5	4	3	4	5
4	2	1	2	4
3	1	$r_{i,j}$	1	3
1	2	1	2	4
5	4	3	4	5

Fig. 2. Hierarchical neighborhood system.

2. Modeling Process

Node selection and task allocation are scheduled by the processing center. The prior knowledge includes the relative position and states of distributed nodes, the frequency range of the target signal, and the last compressed data. According to this prior knowledge, the Markov random field can realize the node state classification, and the purpose of node selection can be realized. The state of the center node is directly related to its transmission attenuation, and the attenuation is greatly affected by geographical conditions. Therefore, the neighboring attenuation is utilized to estimate the selected probability of the center node.

Let node 1, node 2, node 3, and node 4 represent the closest four nodes to the center node [16]. Figure 3 shows a first-order neighborhood system model divided by the processing center for all nodes. In the two-dimensional space $\boldsymbol{R}$, the state set of the node is denoted as $I = \{0, 1\}$, 1 indicates that the node participates in the DMWC system, and 0 means the opposite.

Assume that $x_i \in I$ is the state of the i-th center node, and $x_i \in I$ is the state of the j-th neighboring node. When the number of neighboring nodes with state 1 is less than 2 in the first-order neighborhood system, it is necessary to abandon the center node. The energy function of the

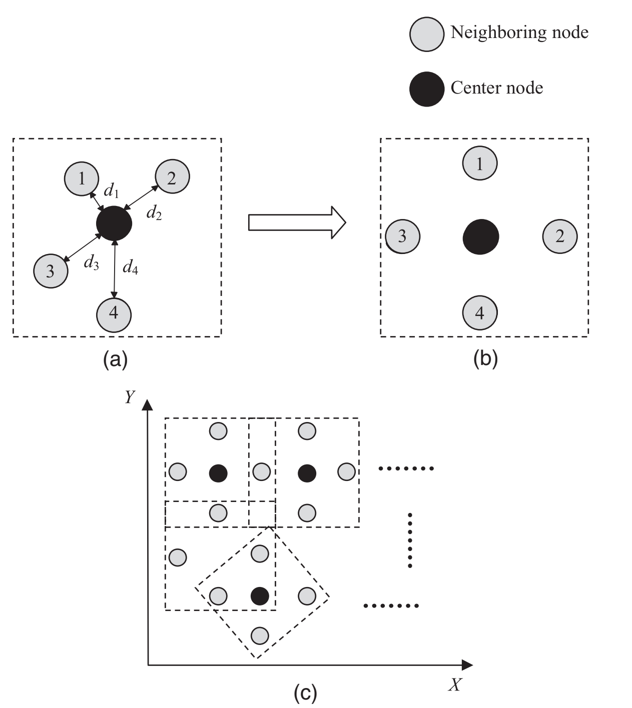

Fig. 3. DMWC node first-order neighborhood system: (a) Original geographic node, (b) equivalent first-order neighborhood system, and (c) global first-order neighborhood system division.

https://doi.org/10.4218/etrij.2017-0028

DMWC first-order neighborhood system can be expressed as

$$U(x) = \sum_{i \in c_1} a_i x_i + \sum_{(i,j) \in c_2} b_{i,j} x_i x_j, \tag{12}$$

where a_i is the self-weight coefficient of the center node, and $b_{i,j}$ is the cross-weight coefficient between the center node and the neighboring node. c_1 is the first-order subgroups, which represents the center node in the DMWC. c_2 is the second-order subgroups, which represents the center node and the closest four neighboring nodes in the DMWC. As long as a_i and $b_{i,j}$ are obtained, the selected probability of the center node can be obtained by substituting the energy function into (11).

The self-weight coefficient a_i is related to the distance from the central node to the signal source and the empirical transmission attenuation of the central node. It is obtained based on prior knowledge in the practical application scenario. The cross-weight coefficient $b_{i,j}$ is related to the neighboring transmission attenuation and the influence ratio of the neighboring node on the center node. The influence ratio can be measured by the distance from the center node to the neighboring node, which is defined as follows:

$$u_j = \frac{\frac{1}{d_j}}{\sum_{j=1}^{4} \frac{1}{d_j}} = \frac{\frac{1}{d_j} \prod_{j=1}^{4} d_j}{d_1 d_2 d_3 + d_1 d_2 d_4 + d_2 d_3 d_4 + d_1 d_3 d_4}, \quad j \in \{1,2,3,4\}, \tag{13}$$

where $d_{j \in \{1,2,3,4\}}$ is the distance from the j-th neighboring node to the center node. The smaller the d_j, the greater the influence ratio u_j, and $u_j \in \{0, 1\}$. To enhance the influence of neighboring transmission attenuation, the cross-weight coefficient $b_{i,j}$ can be modeled using double attenuation coefficient α_i as follows:

$$b_{i,j} = \alpha_j^2 u_j, j \in \{1,2,3,4\}. \tag{14}$$

As defined in (13) and (14), the attenuation coefficient is proportional to $b_{i,j}$, and the distance is inversely proportional to $b_{i,j}$. When (11) and (12) are determined, the auto-logistic model of the Markov random field is degraded into the Ising model owing to the first-order neighborhood system, which is similar to the image segmentation. Thus, the conditional probability can be expressed as

$$P(x_i|x_{c_2}) = \frac{e^{a_i x_i + \sum_{j \in c_2} b_{i,j} x_i x_j}}{1 + e^{a_i x_i + \sum_{j \in c_2} b_{i,j} x_i x_j}}. \tag{15}$$

When considering whether the center node is chosen to join the DMWC, it is necessary to analyze the influence of the self-weight coefficient and cross-weight coefficient on the selection probability. Therefore, since we are only concerned with the state of the center node $x_i = 1$, we calculate the node selected probability as follows:

$$P(1|x_{c_2}) = \frac{e^{a_i + \sum_{j \in c_2} b_{i,j} x_j}}{1 + e^{a_i + \sum_{j \in c_2} b_{i,j} x_j}}. \tag{16}$$

Once the states of all neighboring nodes are known, the DMWC can calculate the selected probability by (16) to determine whether the center node is selected as the virtual undersampling channel.

3. Algorithm of DMWC Node Based on MRF

1) Determine the number of nodes that need to be added based on the time-varying support set.
2) Allocate the neighboring nodes to complete the neighborhood system division according to the prior knowledge from the processing center.
3) Calculate the weight coefficients a_i and $b_{i,j}$ to establish the energy function according to prior knowledge.
4) Calculate the selected condition probability $P(1|x_{c_2})$ of the center node.
5) The processing center selects the center nodes with the largest $P(1|x_{c_2})$ in which to take part. Update the number of geographical network nodes.

The transmission attenuation coefficient has a direct effect on the recovery performance. To verify that the DMWC can avoid the inferior-node high probability using the Markov random field, we define an average transmission attenuation coefficient α_c as follows:

$$\alpha_c = \frac{1}{m'} \sum_{j=1}^{4} \alpha_j, \; m' \geq 2, \tag{17}$$

where α_j is the transmission attenuation coefficient of four neighboring nodes, and m' is the number of neighboring nodes that have taken part in the DMWC. The larger the α_c, the higher the reconstruction rate of the final support set.

IV. Numerical Simulations and Discussion

1. Analysis of Recovery Performance

The number of distributed nodes has an important influence on signal spectrum sensing. When the signal

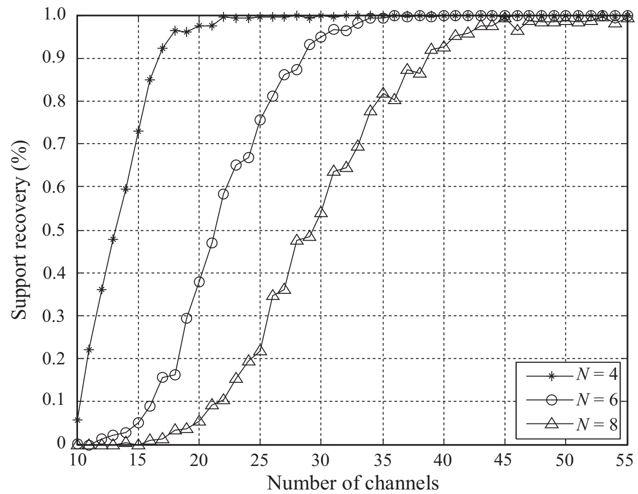

Fig. 4. Curvilinear relation between attenuation coefficient and recovery rate at different SNR levels.

sparsity changes, the DMWC needs to adjust the number of sensing nodes in time to ensure the accuracy of the sensing results. To examine the effect of the node number and signal sparsity on DMWC recovery, we set nodes in the ideal condition with SNR = 20 dB and $\alpha_c = 0.9$. As the signal sparsity increases in Fig. 4, the DMWC needs to increase the number of nodes to achieve the same expected recovery rate.

However, different nodes have different attenuation coefficients. The following experiment examines the influence of different degrees of node attenuation on DMWC signal reconstruction in different SNR regimes. The number of sensing nodes in the simulations is 50. This demonstrates that the larger the α_c, the higher the recovery rate of the final support set in Fig. 5. When the attenuation coefficient is too small, the joint sparsity between all sensing nodes will be destroyed, which makes recovery of the correct support set impossible. Therefore, it is essential for the DMWC to select the sensing nodes with larger attenuation coefficients to realize the spectrum sensing. The following is the process using the MRF to select the ideal sensor node with superior performance.

2. Self-Weight Coefficient and Cross-Weight Coefficient

When the states of four neighboring nodes are all 0, the center node is not affected by the neighboring nodes, and the probability of being selected is only related to a_i. When the states of four neighboring nodes are not all 1, the center node will be greatly affected by the neighboring nodes, and the probability of being selected is related to a_i and $b_{i,j}$.

To select an appropriate a_i in the following sequence, we set the states of the neighboring nodes all to 0 to analyze the influence of a_i on $P(1|x_{c_i})$. As shown in Fig. 6 in the ideal case, the better the self-performance, the higher the probability.

When a large number of distributed nodes are preset in the target geographic area, the distance relationship between the nodes will be determined. As described in Fig. 7 without the influence of self-weight coefficient a_i, the curve is on the rise when the influence ratio u_j increases, namely, the closer the distance from the neighboring node to the center node, the greater the effect on the center node.

In addition, the probability $P(1|x_{c_i})$ is largely determined by the neighboring attenuation coefficient α_j.

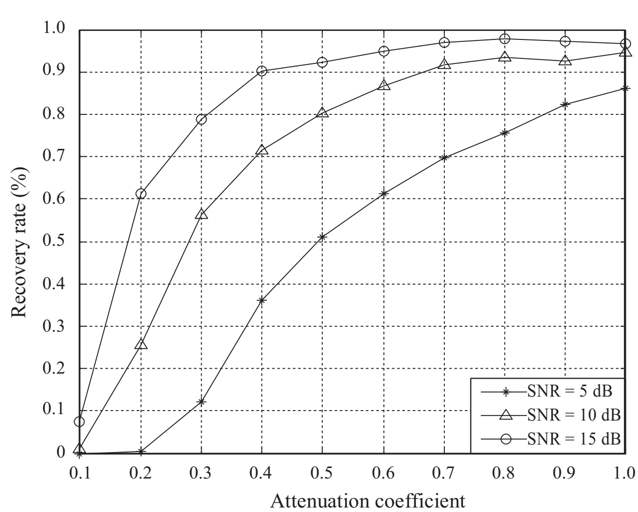

Fig. 5. Curvilinear relation between attenuation coefficient and recovery rate under different SNR levels.

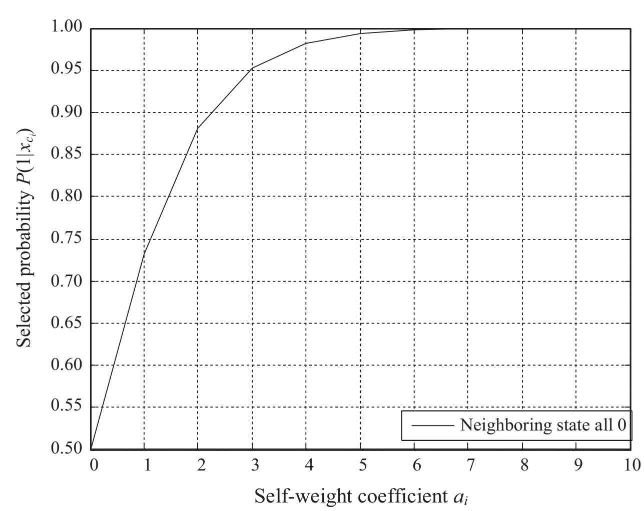

Fig. 6. Relation between self-weight coefficient a_i and probability $P(1|x_{c_i})$.

https://doi.org/10.4218/etrij.2017-0028

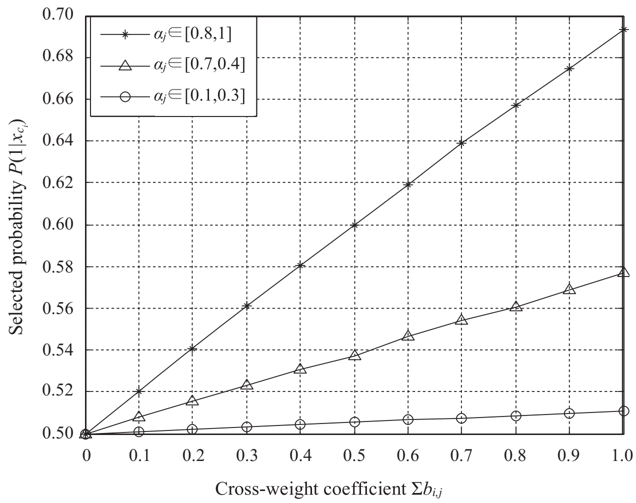

Fig. 7. Relation between influence ratio u_j and probability $P(1|x_{c_i})$ when a_i is 0.

Table 1. Probability of nodes with different attenuations.

State of neighboring nodes				Selected probability ($\alpha_i = 0$)	α_c
Node 1 $\alpha_1 = 0.8$	Node 2 $\alpha_2 = 0.6$	Node 3 $\alpha_3 = 0.3$	Node 4 $\alpha_4 = 0.1$		
0	0	0	0	0.500000	0.00
0	0	1	1	0.506250	0.20
0	1	0	1	0.523109	0.35
1	0	0	1	0.540536	0.45
0	1	1	0	0.528095	0.45
1	0	1	0	0.545499	0.55
1	1	0	0	0.562177	0.70
0	1	1	1	0.528718	0.50
1	0	1	1	0.546119	0.60
1	1	0	1	0.562792	0.75
1	1	1	0	0.567707	0.85
1	1	1	1	0.568320	0.90

Even if the center node is closer to the neighboring nodes, it will not be selected as the undersampling node when the neighboring nodes have worse attenuation coefficients. In Table 1, we assume that the distances from the neighboring nodes to the center node are equal, which means that u_j of the four neighboring nodes have the same effect on $P(1|x_{c_i})$. We can conclude that the larger the average transmission attenuation α_c, the greater the $P(1|x_{c_i})$.

3. Comparison of Recovery Performance

In order to verify the desirable effect of the Markov random field on DMWC node selection, we compared the reconstruction rate using two methods: selection in random and the Markov random field. The simulation signal model is given by

$$x(t) = \sum_{i=1}^{N/2} \sqrt{E_i B} \sin c(Bt) \cos(2\pi f_i t), \qquad (18)$$

where each width B equals 50 MHz. The energy coefficient E_i is random in (0, 10], and the carrier f_i is random within [0, 5 GHz].

In the numerical experiment, we assume that 50 nodes with $\alpha_i \in [0.8, 1)$ have taken part in the DMWC system. Here, we calculate the support reconstruction rate by using 1,000 Monte Carlo simulations. We need to select 10 newly added nodes from first-order neighborhood systems to improve the recovery performance. The number of first-order neighborhood systems is 20. Set 10 of them with the better transmission attenuation interval $\alpha_i \in [0.8, 1)$, and the remaining 10 with the worse transmission attenuation interval $\alpha_i \in [0.3, 0.6)$. If the node is selected at random, the selected probability of the center node is $m'/20 = 0.5$. Assuming that the nodes are uniformly distributed in the sensing region, the processing center chooses the node with the highest probability as the newly added sensing channel, and calculates its average attenuation coefficient, which is estimated according to (17), as a priori knowledge for the next node selection.

In Fig. 8, the line with asterisks indicates that the new node is selected at random, and the line with triangles is the result of selection using the Markov random field model. It can be found that the performance of using the Markov random field goes beyond that of the randomly selected method from Fig. 8.

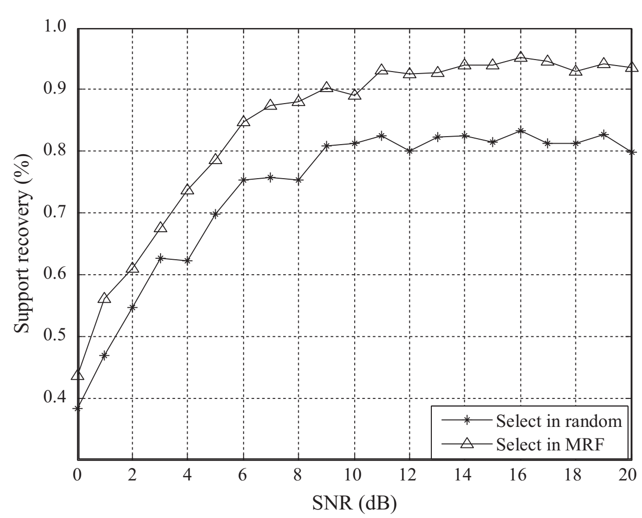

Fig. 8. Comparison of recovery performance in MRF and random at different SNR levels.

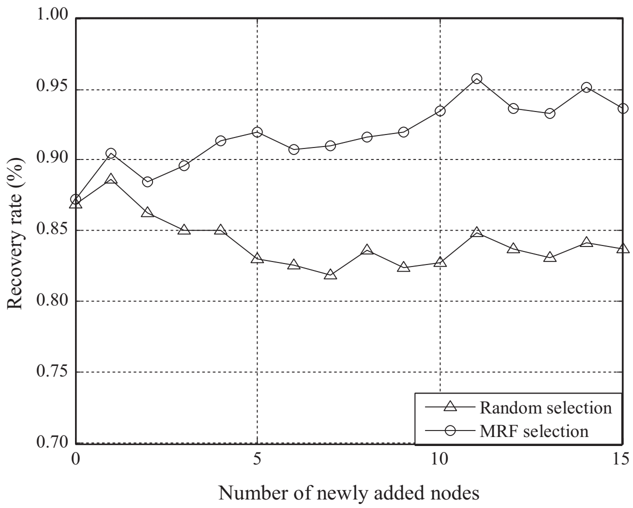

Fig. 9. Comparison of recovery performance in MRF and random by adding nodes.

In order to improve the recovery performance of the DMWC, we examine the effect of MRF selection and random selection on the recovery rate by gradually adding new sensing nodes. Assume that 30 nodes with $\alpha_i \in [0.7, 1)$ have taken part in the DMWC system. The number of first-order neighborhood systems is 30. Set 15 of them in the better transmission attenuation interval $\alpha_i \in [0.8, 1)$, and the remaining systems in the worse transmission attenuation interval $\alpha_i \in [0.3, 0.6)$. All nodes are uniformly distributed in the sensing region with SNR = 20.

As shown in Fig. 9, increasing the number of sensing nodes using the MRF selection can improve the signal reconstruction rate gradually. By contrast, both good and bad nodes are selected to join the DMWC using random selection, so the recovery rate floats up and down at some level. We conclude that random selection can result in a negative effect for DMWC sensing owing to the addition of the poor nodes. Therefore, adopting MRF selection to choose the sensing nodes can effectively avoid the influence of severe attenuation on spectrum sensing.

V. Conclusions

In this paper, we proposed the spectrum sensing of a DMWC based on a Markov Random Field. The method of the Markov random field commonly used in image segmentation was introduced first to realize the node selection when the DMWC increases the number of nodes to improve the performance. We analyzed the selection problem in a first-order neighborhood system, and constructed a suitable energy function using a self-weight coefficient and the cross-weight coefficient. In addition, we explored the influence of the distance and transmission attenuation coefficient on the selection probability. Finally, numerical simulations indicated that the DMWC could improve the reconstruction rate and the anti-noisy performance by using a Markov random field compared with random selection. However, this work only considers a first-order neighborhood system. We need further research on higher orders.

Acknowledgements

This work was supported by the Science and Technology Plan Project of Sichuan Province in China, named Security Collaborative Spectrum Sensing Network Based on The MWC System (No. 2016GZ0091).

References

[1] E. Axell, G. Leus, E.G. Larsson, and H.V. Poor, "Spectrum Sensing for Cognitive Radio: State-of-the-Art and Recent Advances," *IEEE Signal Process Mag.*, vol. 29, no. 3, 2012, pp. 101–116.

[2] R. Jayaprakash and K. Visa, "Cooperative Game-Theoretic Approach to Spectrum Sharing in Cognitive Radios," *J. Signal Process.*, vol. 106, Jan. 2015, pp. 15–29.

[3] M. Moshe and E. Yonina, "From Theory to Practice: Sub-Nyquist Sampling of Sparse Wideband Analog Signals," *JSTSP*, vol. 4, no. 2, Apr. 2010, pp. 375–391.

[4] M. Moshe and E. Yonina, "Blind Multiband Signal Reconstruction: Compressed Sensing for Analog Signals," *IEEE Trans. Signal Process.*, vol. 57, no. 3, Mar. 2009, pp. 993–1009.

[5] M. Moshe and E. Yonina, "Wideband Spectrum Sensing at Sub-Nyquist Rates," *IEEE Signal Process Mag.*, vol. 28, no. 4, 2011, pp. 102–135.

[6] E. Candes and T. Tao, "Near Optimal Signal Recovery from Random Projections: Universal Encoding Strategies," *IEEE Trans. Inform. Theory*, vol. 52, no. 12, Dec. 2006, pp. 5406–5425.

[7] X. Zhang, L. Xiaozhu, S. Hooman, and B. Jalaian, "Cooperative Spectrum Sensing in Cognitive Wireless Sensor Networks," *Int. J. Distrib. Sensor Netw.*, vol. 11, no. 8, Jan. 2015, pp. 1–15.

[8] C. Song and Q. Zhang, "Cooperative Spectrum Sensing with Multi-Channel Coordination in Cognitive Radio Networks," *IEEE Int. Conf. Commun.*, May 23–27, 2010.

[9] X. Ziyong, L. Zhi, and L. Jian, "Broadband Cooperative Spectrum Sensing Based on Distributed Modulated Wideband Converter," *Sensors*, vol. 16, no. 10, Oct. 2016, pp. 1–12.

[10] C. Wei, X. Zhang, J. Liu, and Y. Guan, "Image Segmentation Algorithm Based on Markov Random Field (MRF) for Radiography," *High Power Laser Particle Beams*, vol. 28, no. 12, Dec. 2016, pp. 124001-1–124001-5.

[11] W. Lei and H. Chenxue, "Improved Hierarchical Markov Random Field Algorithm Color Image Segmentation Algorithm," *J. Comput. Appl.*, vol. 36, no. 9, Sept. 2016, pp. 2579–2579.

[12] Y. Zhou, Z. Zhou, and B. Li, "Sensing Nodes Selection and Data Fusion in Cooperative Spectrum Sensing," *IET Commun.*, vol. 8, no. 13, Sept. 2014, pp. 2308–2314.

[13] D. Lee, "Adaptive Random Access for Cooperative Spectrum Sensing in Cognitive Radio Networks," *IEEE Trans. Wireless Commun.*, vol. 14, no. 2, Feb. 2015, pp. 831–840.

[14] Y. Peng, F. Al-Hazemi, H. Kim, and C. Youn, "Joint Selection for Cooperative Spectrum Sensing in Wireless Sensor Network," *IEEE Sensor J.*, vol. 16, no. 22, Nov. 2016, pp. 7837–7838.

[15] T. Wang, M. Yang, and J. Wu, "Distributed Detection of Dynamic Event Regions in Sensor Networks with a Gibbs Field Distribution and Gaussian Corrupted Measurements," *IEEE Trans. Commun.*, vol. 64, no. 9, Sept. 2016, pp. 3932–3945.

[16] R. Versteegen, G. Gimel'farb, and P. Riddle, "Texture Modeling with Nested High-Order Markov-Gibbs Random Fields," *Comput. Vis. Imag. Understand.*, vol. 143, Feb. 2016, pp. 120–134.

Zhi Li received his BS degree in electronics engineering from Shenyang Aerospace University, China, in 1997, and his MS degree in pattern recognition and intelligent systems and his PhD degree in applied mathematics from Sichuan University, Chengdu, China, in 2000 and 2004, respectively. He joined the Autonomus Computing Lab at the University of Arizona, Tucson, USA, in 2013. He is currently a professor at Sichuan University. His research interests include IOT and mobile computing, compressive sensing and spectrum sensing, biomedical signal processing, and medical data analysis technologies.

Jiawei Zhu received her BS degree in electronics engineering from Nantong University, Jiangsu, China, in 2016. She is currently an MS candidate in the Department of Electronics and Information Engineering at Sichuan University, Chengdu, China. Her research interests include compressive sensing and spectrum sensing.

Ziyong Xu received his BS and MS degrees from the Department of Electronics and Information Engineering at Sichuan University, Chengdu, China, in 2014 and 2017, respectively. He is currently a communications engineer in China. His research interests include spectrum sensing and communication systems.

Wei Hua received his BS and MS degrees in radio physics and his PhD degree in biomedical engineering from Sichuan University, Chengdu, China, in 1990, 1998, and 2007, respectively. He is currently a professor at Sichuan University. His research interests include IOT and mobile computing, compressive sensing and spectrum sensing, biomedical signal processing, and microwave chemistry.